Journal of Power Sources 184 (2008) 610–616

Contents lists available at ScienceDirect

Journal of Power Sources

journal homepage: www.elsevier.com/locate/jpowsour

Surface treatment of zinc anodes to improve discharge capacity and suppress hydrogen gas evolution

Yung-Da Cho, George Ting-Kuo Fey*

Department of Chemical and Materials Engineering, National Central University, Chung-Li 32054, Taiwan, ROC

ARTICLE INFO

Article history:
Received 14 January 2008
Received in revised form 27 April 2008
Accepted 29 April 2008
Available online 7 May 2008

Keywords:
Zinc-air batteries
Surface treatments
Lithium boron oxide
Corrosion

ABSTRACT

The shape change and redistribution of zinc anode material over the electrode during repeated cycling have been identified as the main factors that can limit the life of alkaline zinc-air batteries. Li_2O–$2B_2O_3$ (lithium boron oxide, LBO) glass with high Li^+ conductivity and stability can be coated on the surface of zinc powders. The structures of the surface-treated and pristine zinc powders were characterized by XRD, SEM, TEM, ESCA and BET analyses. XRD patterns of LBO-coated zinc powders revealed that the coating did not affect the crystal structure. TEM images of LBO-coated on the zinc particles were compact with an average passivation layer of about 250 nm. The LBO layer can prevent zinc from coming into direct contact with the KOH electrolyte and minimize the side reactions within the batteries. The 0.1 wt.% LBO-coated zinc anode material provided an initial discharge capacity of 1.70 Ah at 0.5 V, while the pristine zinc electrode delivered only 1.57 Ah. A surface-treated zinc electrode can increase discharge capacity, decrease hydrogen evolution reaction, and reduce self-discharge. The results indicated that surface treatment should be effective for improving the comprehensive properties of anode materials for zinc-air batteries.

1. Introduction

The zinc-air battery provides the highest available energy density for any primary battery system [1] and is commonly used for hearing aids and mobile applications. Furthermore, the zinc-air secondary battery has a flat discharge voltage, long shelf life and safety features. It is low cost, non-toxic, more environmentally friendly than many other battery systems, and it can be used within a wide temperature range [1].

The main disadvantage of both primary and secondary zinc-air batteries is their limited cycle life due to degradation of the zinc anode material and carbonation of the KOH electrolyte. Shape change, dendrite shorting, passivation or zinc densification, and hydrogen evolution reaction (HER) of the zinc electrode, have been identified as the principal causes for its poor cycle life [2]. Shape change refers to the reduction of the electrochemically active surface area of the zinc electrode during repeated cycling of the battery, as a result of the redistribution of zinc material over the electrode. These problems have largely been solved by improving separators [3,4] or by using various additives like Bi_2O_3 [5,6], $Ca(OH)_2$ [7,8], Ga_2O_3 [9], $In(OH)_3$ [10,11], PbO [12,13], SnO_2 [13], Tl_2O_3 [11,14], CdO [14], $Mg(OH)_2$ [15], and $Ba(OH)_2$ [15] with the zinc electrode. In some cases, additives like KF [16] or LiOH [17] were added directly into the electrolyte to minimize zinc degradation. The final solution to these problems must come from a thorough understanding of the fundamental phenomena involved in the redistribution of zinc material over the electrode [18–20].

Zinc has a more negative reduction potential than hydrogen, which consequently creates the problem of a hydrogen evolution reaction [21]. This disadvantage makes it difficult for zinc secondary batteries to be commercialized. Many attempts have been made to suppress hydrogen gas evolution. Mercury has been found to be the most effective additive for suppressing HER, but is prohibited from use due to environmental concerns [22–26]. Other additives such as zincate [27], ZnO, V_2O_5, PbO, $(NH_4)_2CS$ [28], and surfactant [29,30] have also been proposed. Yano et al. [31] reported that using zinc particles alloyed with bismuth and lead, and modified with indium, also suppressed hydrogen gas evolution.

In this paper, the surface of zinc particles modified with various wt.% of Li_2O–$2B_2O_3$ (lithium boron oxide, LBO) by a solution process was investigated to clarify its effect on suppressing the hydrogen evolution reaction. In addition, we examined the electrochemical performance of the surface modified zinc electrodes.

2. Experimental

Zinc anode particles were coated with 0.05, 0.1, 1.0, and 2.0 wt.% of LBO by a solution process. LBO was synthesized according to a described procedure from 5.97×10^{-4} mol ethanolic $LiOH{\cdot}H_2O$

* Corresponding author. Tel.: +886 3 425 7325/422 7151x34206; fax: +886 3 425 7325.
E-mail address: gfey@cc.ncu.edu.tw (G.T.-K. Fey).

0378-7753/$ – see front matter © 2008 Elsevier B.V. All rights reserved.
doi:10.1016/j.jpowsour.2008.04.081

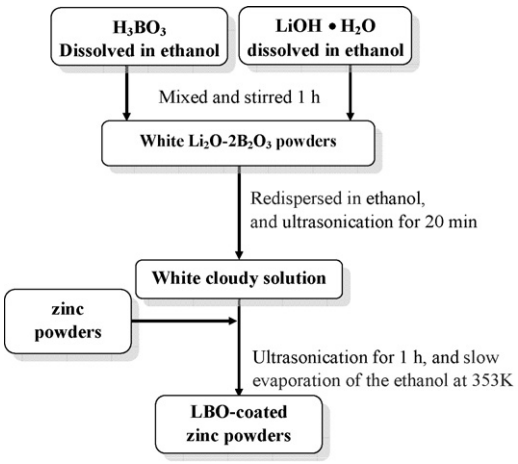

Fig. 1. Schematic of the LBO-coated zinc powders by solution process.

(99%, Aldrich) and 1.19×10^{-3} mol ethanolic H_3BO_3 (98.5%, Aldrich) with constant stirring at 333 K for 1 h to remove excess solvent and form a white LBO powder. The LBO powders were re-dispersed in ethanol and ultrasonicated for 20 min. The 5 g zinc powders (purity: 99.9%, Merck) were added to the above solution and ultrasonicated for 1 h. A subsequent slow evaporation of the ethanol at 353 K resulted in a dark dry mass of the LBO-coated zinc powders. The complete procedure for the synthesis of LBO-coated zinc particles is illustrated in Fig. 1. Zinc electrodes were composed of 95 wt.% LBO-coated zinc powders, 5 wt.% Polytetrafluoro ethylene (PTFE). Electrodes were cast as a slurry in 99% ethanol onto copper current collectors and dried at 60 °C for at least 1 h, the dried coated electrodes roller-pressed with 3 tons pressure for use as anodes.

The corrosion rate can be investigated by volumetric measurement of the hydrogen evolution reaction as a function of time. In this work, a volumetric measurement was used to investigate the hydrogen evolution rate. The apparatus used consisted of a glass vial with airtight cap and a cylindrical graduated Teflon tube fed with paraffin, as shown in Fig. 2 [31]. The volumetric measurement was performed at 323 K. The as-prepared LBO-coated zinc anode active material was packed in a 1.6 cm^2 separator bag, which was placed into a glass vial filled with 25 wt.% KOH. The vial was sealed airtight and connected to a capillary tube containing 10 ml of paraffin. Levels of paraffin were monitored during an 18-day period. As corrosion occurs with subsequent hydrogen evolution, the paraffin level rose as a function of the corrosion rate.

Structural properties of the LBO-coated zinc materials were studied by the X-ray diffraction method (Siemens D5000). Diffraction patterns were acquired with nickel-filtered Cu Kα radiation between scattering angles of 15° and 80° in increments of 4°. The depth profiles of lithium, boron, oxygen and zinc were recorded by an electron spectroscopy for chemical analysis (ESCA) instrument (VG Scientific ESCALAB 250) with monochromatic Al Kα radiation of 1486.6 eV. The morphology and size of the particles were examined by scanning electron microscopy (Hitachi model S-3500V) and transmission electron microscopy (JEOL JEM-200FXII). The LBO coating was confirmed with energy dispersive spectroscopy (energy dispersive X-ray spectrometry). BET surface area was measured by the nitrogen adsorption–desorption method (Micromeritics ASAP 2010).

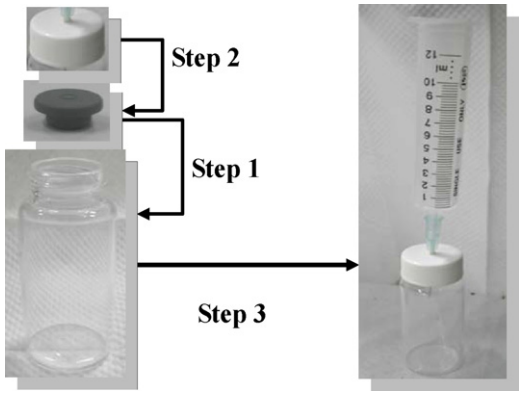

Fig. 2. Apparatus for measuring hydrogen gas evolution.

The alkaline zinc-air cell was assembled in a nitrogen-filled glove box. Fig. 3 is the apparatus of the alkaline zinc-air cell. The cell consisted of two rectangular shaped Teflon casing containers, 5 cm in length and 3.5 cm in breadth, that sandwiched the components of the cell in the order: a LBO-coated zinc electrode functioning as an anode (2.6 cm × 1.5 cm × 0.3 cm), a Celgard 2216 separator microporous polypropylene membrane (2.6 cm × 1.5 cm × 0.01 cm) being soaked in a 25 wt.% KOH solution, and a carbon-based commercial air cathode (2.6 cm × 1.5 cm × 0.15 cm) that was sufficiently porous and permeable to air. Furthermore, an acrylic plate, which had an volume of 4.45 cm^3 (3.3 cm × 1.5 cm × 0.9 cm) with 18 small holes (diameter 0.3 cm), was placed next to the cathode to allow limited air passing. To avoid self-discharge of zinc in contact with air, the acrylic plate was kept closed until the cell was ready to discharge. The alkaline zinc-air cell was operated at an applied current of 0.64 A and a discharge cut-off voltage of 0.5 V in a multi-channel battery tester (Arbin, BT 2000) at 298 K.

3. Results and discussion

3.1. Gassing testing

The need to suppress hydrogen formation is critical for both primary and secondary zinc-air batteries. Although mercury has been an effective additive for this purpose, it is prohibited due to its environmental toxicity. Other less-toxic alternative additives such as ZnO and sodium dodecyl sulfate (SDS) have been proposed [27,30]. In general, the rate of hydrogen evolution reaction (HER) greatly depends on the hydrogen overpotential of the zinc anode materials. In order to study the additive effect on HER, the hydrogen volume evolved from the as-prepared LBO-coated zinc particles were measured by a volumetric method. Fig. 4 shows the results of the measurements of hydrogen evolution volume during zinc corrosion. Fig. 4 displays a significant difference in gassing behavior between the bare zinc and various LBO-coated zinc powders. It is evident that zinc corrosion was quite intensive without the use of any additive and the volume of hydrogen evolution was approximately 3.75 times higher that for the optimal coating composition of 0.1 wt.% LBO-coated zinc powders. The remarkable effect of suppressing HER by LBO coating on zinc powders was due to the fact that the surface of the zinc particles was protected by the LBO layer which provided a passivation layer to prevent direct contact of zinc with the electrolyte. At higher coating levels of 1.0 and 2.0 wt.% LBO, it is difficult to form a homogeneous coating layer, as can be observed from TEM analysis. However, the hydrogen evolution of 0.1 wt% LBO added zinc reached almost 10 ml after 16 days which is about 80 % of the bare zinc sample. It might cause the easy dissolution of the Li_2O–$2B_2O_3$ coating layer in high concentration KOH solution. Table 3 which shows the ICP-AES results of 25 wt.% KOH electrolyte after discharge testing. There were some Li and B components in the electrolyte and a LiOH composition could have formed which stabilized the supersaturated discharge product

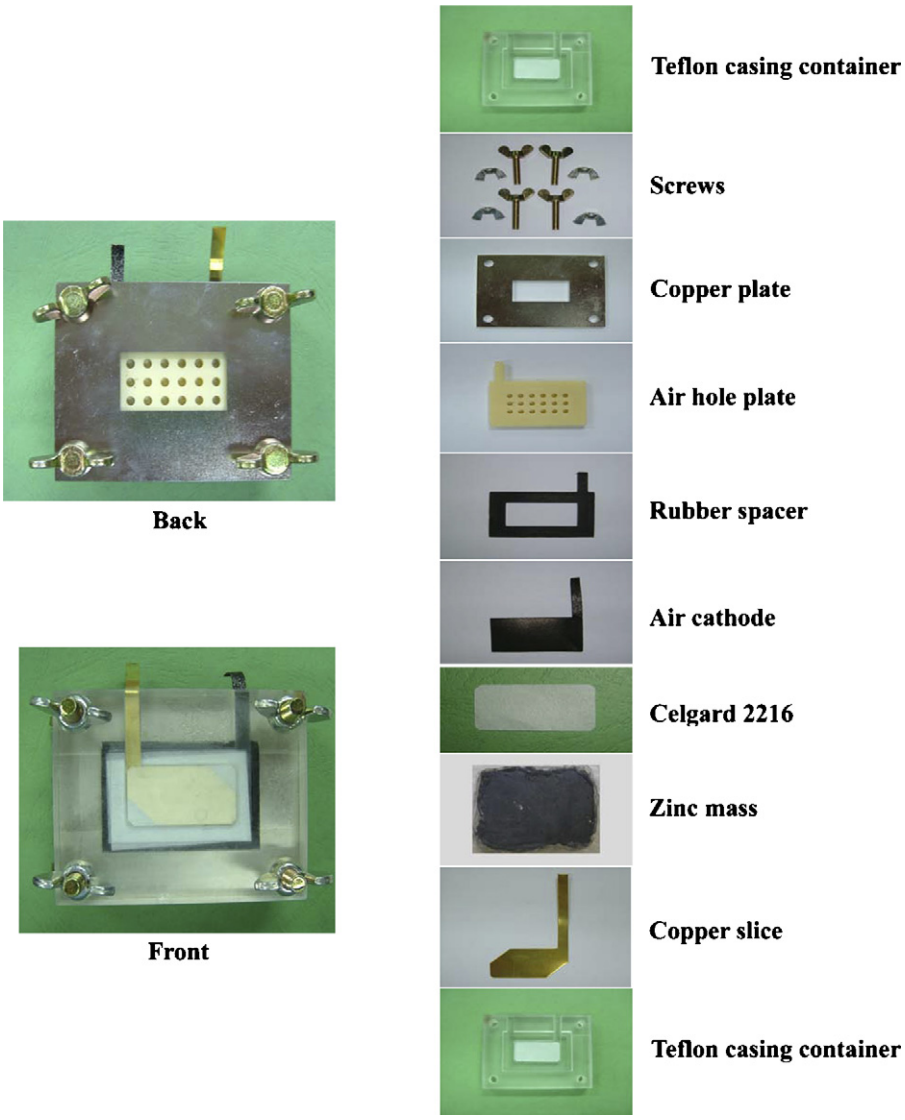

Fig. 3. Assembly of the alkaline zinc-air cell.

zincate solution [32,33] and may have decreased the dissolution of the zinc anode, which would have been beneficial to electrochemical properties.

3.2. X-ray diffraction

Fig. 5 shows the XRD patterns of the pristine, 0.1 wt.% LBO-coated, and JCPDS of zinc powders. The diffraction patterns conformed to the Hexagonal structure of the core zinc metal, but the absence of patterns corresponding to LBO may be due to very low concentrations of LBO that might have formed on the surface of the core material and/or its amorphous (glassy) structure. The XRD patterns of the LBO-coated particles showed no basic change, and did not form a solid solution by interacting with core zinc metal. This result is supported by ESCA data and TEM images presented in a later section.

3.3. ESCA

The spatial distributions of Zn, Li, B and O in the LBO-coated zinc powders were examined by an ESCA depth profile analysis. The results of the analysis on 0.1 wt.% LBO-coated zinc particles are displayed in Fig. 6 and Table 1. It can be seen that the concentration of Li, B and O dropped from the coating surface to nearly zero at the core zinc metal. The depth of the LBO layer was around 250 nm, which was consistent with the coating thickness observed

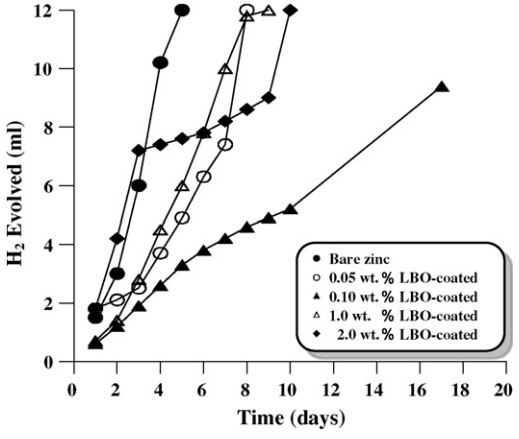

Fig. 4. Hydrogen gassing vs. time for the various wt.% of LBO-coated zinc powders.

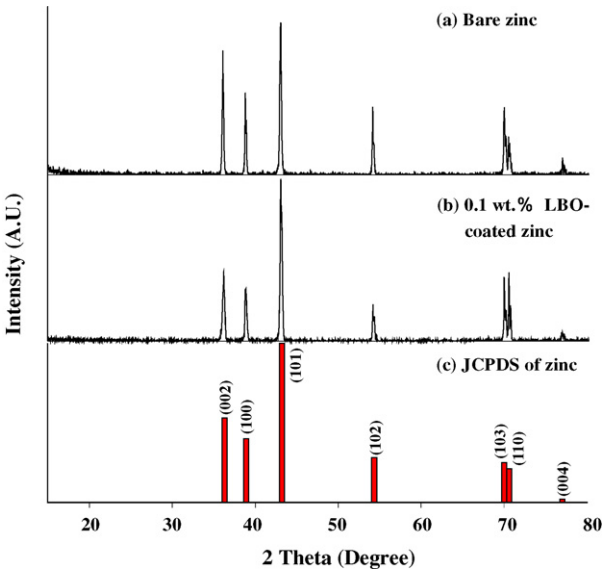

Fig. 5. X-ray diffraction patterns of (a) bare zinc particles, (b) 0.1 wt.% LBO-coated zinc particles, and (c) JCPDS of zinc particles.

Table 1
Elemental analysis for the surface of bare and 0.1 wt.% LBO-coated zinc powders

Samples	Composition (at.%)			
	Zn	Li	B	O
Bare Zn powders	99.87	0	0	0.13
0.1 wt.% LBO-coated zinc powders	0.04	14.62	24.47	60.87

from the TEM study. The high atomic concentration of oxygen at the surface of the zinc powders was reasonable due to the presence of oxygen in LBO and possibly also the native oxide film on the starting Zn particles. Below the coating layer, there was a rapid decrease in Li concentration along the depth of core zinc metal. Therefore, it is clear from depth profile analysis that the Li, B and O elements were distributed only on the surface of zinc powders, and did not form any solid solution phase, which corroborates our XRD results.

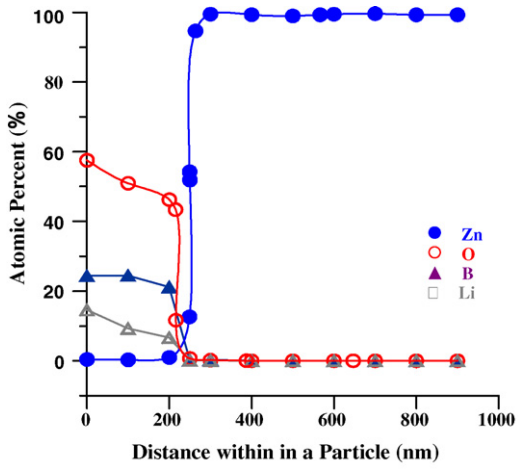

Fig. 6. ESCA depth profiles of lithium, boron, oxygen, and zinc in 0.1 wt.% LBO-coated zinc powders.

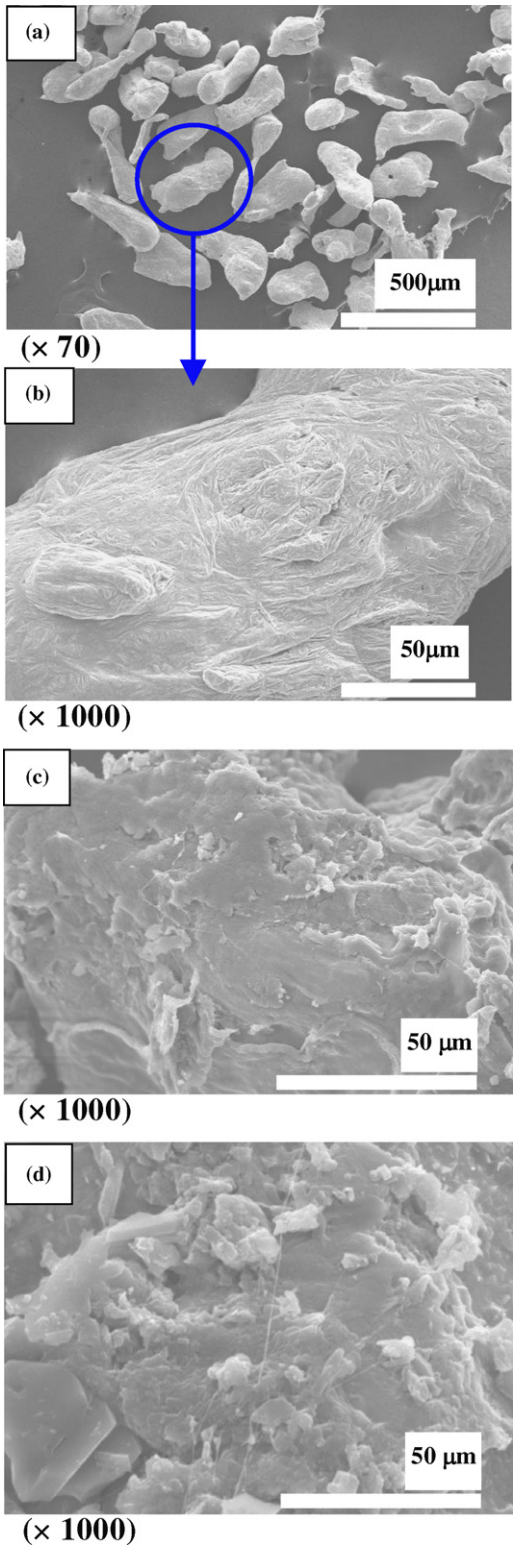

Fig. 7. SEM micrographs of (a) bare zinc particles, (b) amplification of the (a), (c) 0.1 wt.% LBO-coated zinc particles, and (d) 2.0 wt.% LBO-coated zinc particles.

3.4. Morphology

Fig. 7 compares surface morphology of the bare, 0.1 and 2.0 wt.% LBO-coated zinc powders. Fig. 7a and b shows that a rough surface was present for the bare zinc particles, and particle size was about 100–400 μm. It can be seen clearly in Fig. 7c that the surface texture

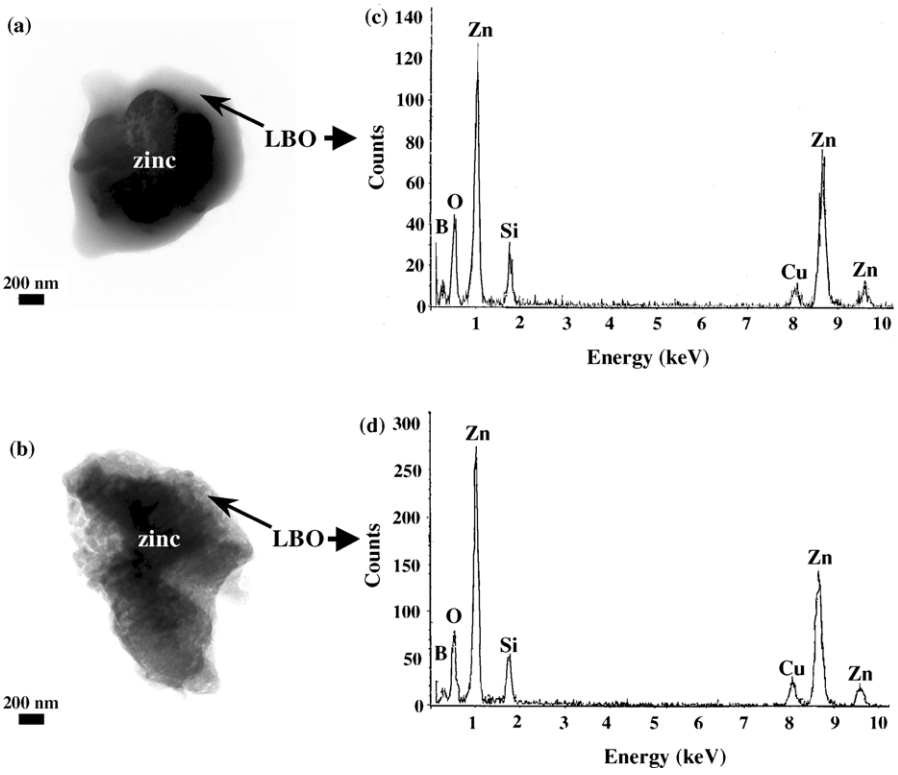

Fig. 8. TEM images and EDS analyses of the LBO-coated zinc particles, (a) and (c) 0.1 wt.% LBO-coated zinc; (b) and (d) 2.0 wt.% LBO-coated zinc.

of the zinc particles was changed and a smooth surface was formed after coating with 0.1 wt.% LBO deposited on the surface of the zinc particles. At higher LBO coating concentrations, such as 2.0 wt.%, as shown in Fig. 7d, the surface was not covered completely by LBO and part of the surface had aggregates of some irregular shaped crystallites displayed in the TEM image of Fig. 8. Undoubtedly, this type of structure facilitated the diffusion of zinc ions into the KOH bulk solution and the penetration OH^- ions into the zinc surface. As a result, the anodic dissolution of zinc could proceed continuously and increase the amount of hydrogen gas evolution until zinc was completely consumed. This is why lower LBO coating concentration was used in our study.

In order to improve our understanding of morphology at a nanostructural level, we performed TEM/EDS analyses of the surface-coated zinc particles, as shown in Fig. 8. The TEM images of 0.1 and 2.0 wt.% LBO-coated zinc particles are shown in Fig. 8a and b, respectively. Their corresponding EDS analyses are displayed in Fig. 8c and d. A 200-mesh copper grid coated with a silicon monoxide film was used as a sample holder. Thus, Cu and Si peaks were present as impurities or background in the EDS spectrum. The 0.1 wt.% LBO-coated zinc particles (Fig. 8a) provided complete coverage and a very thin film that covered the surface of the zinc particles (dark opaque region).

The thickness of the LBO coating layer in Fig. 8a was around 250 nm, which identity was confirmed to be LBO by EDS analysis of Fig. 8c. The 2.0 wt.% LBO-coated zinc particles (Fig. 8b) showed remarkable aggregation and uneven coating on the surface of the zinc particles. Thus, it appears that a coating level of 0.1 wt.% would be sufficient to form an adherent and a complete protective coverage. Therefore, the reducing amount of hydrogen gas evolution can be attributed to the thin and uniform LBO passivation layer. Similar passivation behavior has been reported by Arnold and Assink who used a polymer film to prevent direct contact between the electrode and the electrolyte, and decrease the dissolution of Zn in the electrolyte [34].

The BET surface area of the bare zinc particles was 0.0316 $m^2\ g^{-1}$. The surface areas of the 0.1 and 2.0 wt.% LBO-coated particles were 0.0120 and 0.1511 $m^2\ g^{-1}$, respectively. The larger surface area of the 2.0 wt.% LBO-coated powders compared to other low wt.% LBO-coated samples was attributed to the larger specific surface area of aggregated LBO coating particles, as shown in Fig. 7b, which in turn increased the surface area of the zinc anode electrode.

3.5. Electrochemical properties

It is well known that zinc utilization decreases very rapidly with decreasing OH^- concentration [35]. This is due to the lower solubility of the discharged product of $Zn(OH)_2$ in diluted KOH solution, which leads to a supersaturation of zincate ions. In order to study the effectiveness of our coating process, we used zinc-air test cells to calibrate the discharge capacity of zinc and study the effects of various wt.% LBO coatings on the discharge capacity of zinc utilization. The cell was discharged in 3 h at an applied current of 0.64 A to a cutoff voltage of 0.5 V. Typical results are shown in Fig. 9 and Table 2. The best LBO-coated zinc electrode was 0.1 wt.% with an initial voltage of 1.44 V, discharge capacity of 1.70 Ah for 159 min and depth of discharge about 89% of the theoretical value. The bare zinc electrode had an initial discharge capacity of 1.57 Ah for 147 min and depth of discharge of about 82%. The enhanced discharge capacity and time could be attributed to the formation of a thin LBO coating layer on the surface of the zinc particles that can prevent Zn from coming into direct contact with the KOH electrolyte and minimize the side reactions within the batteries. The discharge capacity of the zinc anode decreased at higher levels of LBO coating due to an increase of electro inactive LBO component in the electrode (Table 3).

Table 2
Capacity vs. time for Zn-air cells containing various wt.% LBO-coated zinc anodes discharged at 0.64 A to 0.5 V discharge cut-off voltage in 25 wt.% KOH solution

	Initial voltage of discharge (V)	Discharge capacity (Ah)	Work voltage (V)	Time of discharge (min)	Depth of discharge (%)
First experimental					
Bare-zinc	1.42	1.57	0.94	147	82
0.05 wt.% LBO-coated	1.42	1.61	0.93	151	84
0.1 wt.% LBO-coated	1.44	1.70	0.94	159	89
1.0 wt.% LBO-coated	1.43	0.35	0.94	33	18
2.0 wt.% LBO-coated	1.43	0.29	0.93	21	11
Second experimental					
Bare-zinc	1.43	1.51	0.93	140	79
0.05 wt.% LBO-coated	1.42	1.58	0.93	145	83
0.1 wt.% LBO-coated	1.42	1.68	0.94	156	88
1.0 wt.% LBO-coated	1.42	0.43	0.93	41	23
2.0 wt.% LBO-coated	1.41	0.19	0.93	17	9

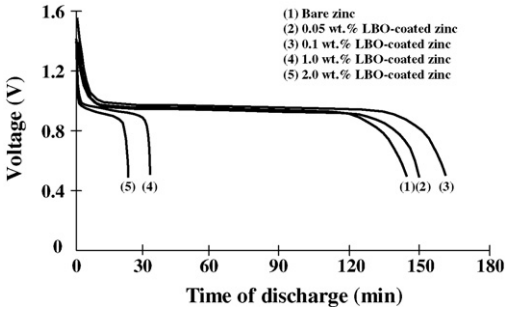

Fig. 9. Discharge curves of cells with bare and LBO-coated zinc electrode at 0.64 A and a 0.5 V and 25 wt.% KOH electrolyte.

3.6. Cyclic voltammetry

Fig. 10a and b show the cyclic voltammograms of bare zinc and LBO-coated zinc, respectively, between −1.90 and 1.0 V at a scan rate of 100 mV s^{-1} in 25 wt.% KOH (5.4 M) solution. In Fig. 10a, there were three peaks: the anodic peak *A* at −1.01 V, the anodic peak *B* at −0.97 V, and the cathodic peak *C* at −1.48 V vs. Hg/HgO. In the anodic sweep, bare zinc was oxidized and formed a $Zn(OH)_4^{2-}$ species, which had a redox potential very close to that for zinc oxidation to ZnO or $Zn(OH)_2$ [36]. In other words, zinc was first oxidized to $Zn(OH)_4^{2-}$ and then readily converted to ZnO or $Zn(OH)_2$ passivation film. The peak *B* observed at −0.97 V in the cathodic sweep was due to further dissolution of the passivated film of ZnO or $Zn(OH)_2$ to a $Zn(OH)_4^{2-}$ species [36]. The redox behavior was similar to what was seen in the voltammograms of the zinc electrode in a 1.0 M KOH solution at a sweep rate of 5 mV s^{-1}, as reported by Cai and Park [36].

The cyclic voltammogram of LBO-coated zinc in Fig. 10b displays that the anodic peak *A*′ of zinc oxidation to $Zn(OH)_4^{2-}$ species shifted positively to −0.50 V, because zinc was more difficult to oxidize when protected by an LBO-coating, which resulted in less hydrogen evolution and a reduced self-discharge. In addition, the voltage separation between peaks *A* and *B* and peaks *A*′ and *B*′ did not change, indicating that the redox behavior of peaks *A*′ and *B*′ was similar to that of peaks *A* and *B*. The current density of peak *B* at −0.97 V was much more intense than that of peak *B*′ at −0.46 V. This revealed that the bare zinc electrode had a thicker passivation layer of ZnO or $Zn(OH)_2$ than the LBO-coated zinc electrode. Dissolution of the passive film results in a loss of zinc active materials, and leads to capacity loss and shorter lifespan for the batteries. Peaks *A* and

Table 3
Results of ICP-AES analysis of the 25 wt.% KOH electrolyte after discharge testing

Samples	Composition (wt.%)		
	Li	B	Zn
Bare-Zn	0	0	100
0.1 wt.% LBO-coated Zn	0.47	0.85	98.68

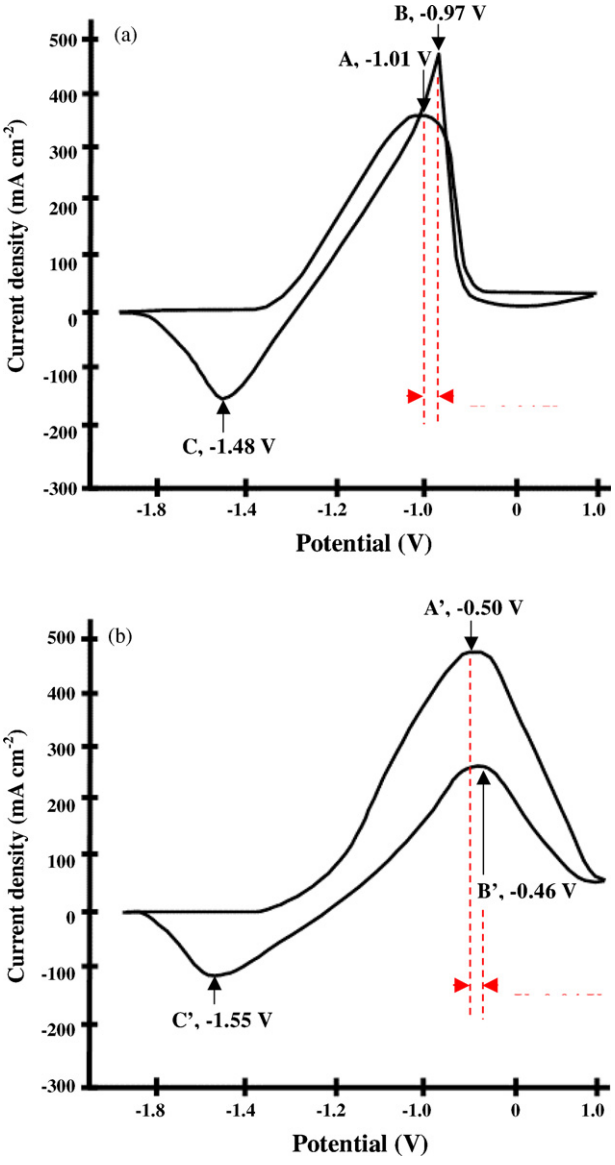

Fig. 10. Cyclic voltammogram of (a) bare zinc electrode and (b) LBO-coated zinc electrode in 25 wt.% KOH. Scanning rate of 100 mV s^{-1}.

C (or peaks *A*′ and *C*′) were conjugated, indicating that peak *C* (or peak *C*′) was ascribed to the reduction of the Zn(II) species to Zn(0).

4. Conclusion

Electron microscopic images revealed that a coating layer with various wt.% LBO was successfully coated over the surface of zinc particles by a solution method. The XRD pattern of the LBO-coated zinc particles without other phases present also indicated that the LBO was only coated on the surface. The 0.1 wt.% LBO-coated zinc anode material used in the zinc-air battery improved cell discharge capacity to 1.70 Ah compared to 1.57 Ah delivered by the pristine zinc anode. The suppression hydrogen evolution reaction effect is believed to be the result of LBO coating, which produces a thin, porous, passive film at the zinc surface. This surface modification of the material structure greatly facilitates the diffusive transportation of discharged product and solution reactant, and thereby improves the anodic utilization of the zinc anode.

Acknowledgement

Financial support by Evionyx Company of Taiwan under grant 931050 is gratefully acknowledged.

References

[1] D. Linden, T.B. Reddy, Handbook of Batteries, 3rd ed., McGraw-Hill, 2002, Chapter 13.
[2] E. Frackowiak, J.M. Skowronski, J. Power Sources 73 (1998) 175.
[3] Sanyo Electric Co., Ltd., Jpn. Pat. 57,162,275 (1982).
[4] Y. Kiros, J. Power Sources 62 (1996) 117.
[5] J. McBreen, E. Gannon, J. Power Sources 15 (1985) 169.
[6] K. Aizawa, Y. Shirogami, H. Yosushi, T. Takamura, Jpn. Kokai Tokkyo Koho, 78,73,332 (1978).
[7] S. Sekido, T. Ohhira, T. Yogoyama, Y. Ikeda, Jpn. Kokai, 75,09,725 (1975).
[8] J.-S. Chen, L.-F. Wang, J. Appl. Electrochem. 26 (1996) 227.
[9] L.Y. Gun'ka, N.G. Nikhalenko, V.N. Flerov, Zh. Prikl. Khim. 54 (1981) 77.
[10] S. Furukawa, M. Nogami, M. Todokora, Jpn. Kokai Tokkyo Koho JP 03,122,235 (1991).
[11] S. Furukawa, S. Murakami, Jpn. Kokai Tokkyo Koho JP 60,185,373 (1985).
[12] K. Okabe, Y. Eguchi, T. Astuda, K. Fujii, Jpn. Kokai Tokkyo Koho JP 04,126,356 (1992).
[13] J. McBreen, E. Gannon, Electrochim. Acta 26 (1981) 1439.
[14] J. McBreen, E. Gannon, J. Electrochem. Soc. 130 (1983) 1980.
[15] F.R. McLarnon, E.J. Cairns, J. Electrochem. Soc. 138 (1991) 645.
[16] J.T. Nichols, F.R. McLarnon, E.J. Cairns, Chem. Eng. Commun. 37 (1985) 355.
[17] Sanyo Electric Co., Ltd., Jpn. Pat. 59,167,970 (1984).
[18] R.G. Gunther, R.M. Bendert, J. Electrochem. Soc. 134 (1987) 782.
[19] L. Binder, W. Odar, J. Power Sources 13 (1984) 9.
[20] Y.-C. Chang, G. Prentice, J. Electrochem. Soc. 131 (1984) 1465.
[21] M. Pourbaix, Atlas of Electrochemical Equilibria in Aqueous Solutions, Pergamon, London, 1966.
[22] K.V. Kordesch, Batteries, vol. 1, Marcel Dekker, New York, 1974, p. 324.
[23] T.D. Dirkse, R. Timmer, J. Electrochem. Soc. 116 (1969) 162.
[24] L.Z. Vorkapic, D.M. Drazic, A.R. Despic, J. Electrochem. Soc. 121 (1974) 1385.
[25] M. Yano, M. Nogami, I. Yonezu, K. Nishio, Y. Akai, M. Kurimura, Denki Kagaku 65 (1997) 154.
[26] A. Miura, K. Takada, R. Okazaki, H. Ogawa, T. Uemura, Y. Nakamura, N. Kasahara, Denki Kagaku 57 (1989) 459.
[27] V. Ravindran, V.S. Muralidharan, J. Power Sources 55 (1995) 237.
[28] R. Shivkumar, G.P. Kalaignan, T. Vasudevan, J. Power Sources 75 (1998) 90.
[29] H. Yang, Y. Cao, X. Ai, L. Xiao, J. Power Sources 128 (2004) 97.
[30] R.K. Ghavami, Z. Rafiei, J. Power Sources 162 (2006) 893.
[31] M. Yano, S. Fujitani, K. Nishio, Y. Akai, M. Kurimura, J. Power Sources 74 (1998) 129.
[32] N.N. Flerov, J. Appl. Chem. (USSR) 30 (1955) 1326.
[33] N.N. Flerov, J. Appl. Chem. (USSR) 33 (1960) 134.
[34] C. Arnold Jr., R.A. Assink, J. Membr. Sci. 38 (1988) 71.
[35] K. Bass, P.J. Mitchell, G.D. Wilcox, J. Smith, J. Power Sources 39 (1992) 273.
[36] M. Cai, S.M. Park, J. Electrochem. Soc. 143 (1996) 2125.